A Framework for 3D Geospatial Buffering of Events of Interest in Critical Infrastructures

Nils Kalstad Svendsen[1] and Stephen D. Wolthusen[1,2]

[1] Norwegian Information Security Laboratory, Gjøvik University College, P.O. Box 191, N-2802 Gjøvik, Norway
[2] Information Security Group, Department of Mathematics, Royal Holloway, University of London, Egham Hill, Egham TW20 0EX, UK

Abstract. The interdependencies among critical infrastructures are frequently characterized not only by logical dependencies and resource flows but often also require consideration of geospatial interactions among the infrastructure elements and surroundings such as the terrain, properties of the terrain, and of events involving the infrastructure such as fire and flooding. Modeling such events and interactions also requires the use not only of three-dimensional geospatial models but also a more precise characterization of both events and the interaction of events with the geospatial model to capture e.g. the resistance of different terrain features to blasts. In this paper we therefore present an extension to a graph-based model reported previously which allows the consideration of geospatial interdependencies and interactions in a specific area of interest. The model incorporates physical characteristics of both the infrastructure elements itself and of terrain and environment in a three-dimensional framework allowing for detailed analyses which cannot be captured using simpler spatial buffering techniques as found in many geospatial information systems.

Keywords: Infrastructure Models, Geospatial Information Systems, Infrastructure Interdependency Analysis, Infrastructure Planning

1 Introduction

When planning critical infrastructures or carrying out disaster management knowledge of the geography of the disaster zone and its surrounding is highly relevant. Awareness of surrounding infrastructures, plausible disaster scenarios, and how infrastructures influences and interacts with each other in different scenarios is utterly important in critical infrastructure design or when managing a disaster scenario. Geographical information systems (GIS) can provide modeling, manipulation, management, analysis, and representation of geographically referenced data, thus providing a powerful tool in a CIP setting. However these systems do not provide an interface to model the functionality of interdependent infrastructures.

The consideration of geospatial information in the assessment of events relating to and for the planning of critical infrastructures therefore adds an important dimension to interdependency analyses based on purely topological interrelations as reported previously [1–4]. While computational complexity constrains the scope of such analyses, the combination of the aforementioned techniques with an approach taking into account geospatial and terrain information can yield highly relevant information that even a straightforward analysis in a two-dimensional environment will not uncover (e.g. in case of terrain features affecting interactions between infrastructure elements or events). Buffering, the formation of areas containing locations within a given range of a given set of feature, is a well known and frequently used GIS technique (see e.g. [5]). The traditional application is to indicate metric or temporal distance to a point given e.g. a topology or road system. Extending buffering to three dimensions and to contain not only topology information but also geospatial objects, that is spatial objects with a well-defined position, will allow to define buffer areas indicating e.g. fire or blast damage, flooded or contaminated area, given that every object is assigned a set of properties indicating permeability to the event.

In combination with the simulation mechanisms reported in earlier research, where we focus on methods for detection of critical interdependencies between networks carrying different types of resources [1–4], three-dimensional geospatial buffering can provide a powerful tool for scenario analysis. Geospatial proximity can itself be classified as a dependency between network components. However, a naïve consideration of proximity can result in both overly conservative estimates (e.g. if a flood barrier lies between an overflowing region and an infrastructure element to to be protected) and missing critical interdependencies induced by terrain features. It is therefore desirable to perform a more detailed local analysis to ensure that the estimations provided by proximity measures over georeferenced nodes in the graph-based model are indeed accurate or require further refinement. This allows both the consideration of interdependencies and threats independent of the topological analysis provided by the graph-based model and also feedback into the graph-based model. This more accurate sub-model can be enhanced further in its accuracy by including a global time base (as opposed to a partial order), which also is feasible mainly in the context of a small regional model. The remainder of this paper is structured as follows: Section 2 describes the geospatial model and several buffering approaches as well as the modeling of permeability to event types, which is then exemplified in a sample scenario in section 3 before a brief review of related work in section 4. Finally, section 5 concludes the paper with a review of current and ongoing work on the proposed model, discussion of the results, and further extensions and refinements in progress.

2 A Framework for 3D Geolocational Buffering

The 3D geolocational buffering we are concerned with requires the introduction of both volume and time-dependent features, and is therefore an extension of more common definitions found in GIS environments. In the following geolocational buffering thus defines a time dependent contamination or destruction area (2D) or volume (3D) surrounding a point, line, or polygon-shaped event source.

The classical GIS approach to 3D buffering is among other places described in [6]. This is often a static approach where uniform conditions are considered around a source. Consider e.g. the description of point buffering in [6]. A point is defined by the coordinate triplet (x, y, z) and its buffering zone is generated by a fixed distance, creating a sphere in the three-dimensional sphere. The sphere generation begins with the creation of a polygon surface, the main circle in the (x, y) plane. Later five circles with diminishing radii are created on the upper and lower side (following the z-axis) of the main circle. This approach leaves no room for variations in propagation speed from the source. Applying this in a CIP scenario we could for example find that a road accident can damage a fiber-optic cable 1.5m under the ground — merely because it is within the blast radius of a road accident involving a tanker truck.

For CIP applications this approach neglects some critical features. In particular we are most interested in knowing what kind of obstacles lie between the source and the edge of the buffer zone. Without this knowledge, the buffer zone becomes a theoretical worst-case scenario which does not take natural or man-made protections into account. The main objective of our work is therefore to determine whether one infrastructure constitutes a threat to another, but it makes no sense to say that a gas line constitutes a threat to a power line if they are on different sides of a hill or that a flooding river is a threat to the surrounding infrastructure if the river runs in a deep ravine. In order to enable such considerations we choose a dynamic approach based on cylindrical or spherical coordinates and partition of the "event sphere" into spherical sectors. This allows detection of eventual obstacles between an event source and eventual points of interest. At the core of any model is the discretization of a continuous phenomenon and translation of physical phenomenons to relations between the modeled objects. After an introduction the physical features and modeling principles of geospatial buffering this section introduces a 2D point source, a 3D point source and a 3D line source buffer model. In this paper, the emphasis is therefore placed on space discretization and the algorithmic steps taken in each iteration.

2.1 Physical Features

The number of parameters and physical scope (albeit reduced significantly over a more abstract regional or national model) of the model requires the use of several approximations so as to obtain a model of suitable computational complexity. Most critical infrastructures considered here are physical infrastructures such as cables and pipelines. Such infrastructure can be damaged or destroyed in numerous ways. This can be natural phenomena (e.g. storms or fire), human actions (e.g. excavations, sabotage, or terrorist acts), or accidents in other infrastructure (e.g. a pipeline blast causing pressure waves and fires). All these events can be modeled in detail. Cables has a certain elasticity which provides a threshold for breaking, fires can be modeled based on material and heat capacities, and pressure waves from an explosion can be modeled based on the amount of explosives and their properties. Including all these features in a model gives us a model of not only high computational complexity, but also creates a long initiation time for each scenario, where not all of the information may be available. We are therefore aiming at a model that can be initiated based on topological information and high-level geospatial information – such as type of vegetation (grassland, trees or asphalt) and human created infrastructure (houses, walls, bridges and tunnels). Then we aim at creating a buffer around some source based on an analysis determining whether it is likely that the incident will cover this area within a certain time with the primary intent being on supporting planning and decision-making, not detailed outcome analysis as may be required for engineering aspects.

2.2 Modeling principles

We assume that a appropriate polygon mesh 3D representation is provided by a GIS tool. In addition to geographic information and spatial information of the type described above must be available. This includes infrastructure, buildings, ground properties (terrain formations), vegetation, and certain properties of these. These objects are are named geospatial objects, and constitute a a group $\mathcal{O}$. Further a set of events is defined. We start by defining a set $\mathcal{S}$ of events that are of interest in a CIP, this can for example be fire, explosions, flooding, leakage of chemical toxic liquids or fluids. An event can originate from different types of sources: point source (e.g. fire or explosion), line source (e.g. pipeline leakage) or polygon source (e.g. flooding). Each element o_i of $\mathcal{O}$ is assigned a resistance parameter ρ_{ij}, describing how resistant the element o_i is to event j. The parameter ρ can be of different nature and granularity. In order to achieve our goal of simplicity in this paper (the model extends naturally to include a resistance function) we state that

$$\rho_{ij} = \begin{cases} 0 & \text{if } o_i \text{ is not resistant to event } j \\ 1 & \text{if } o_i \text{ is resistant to event } j. \end{cases}$$

Based on this classification of the objects in the model our approach is based on an discretization of time and space. For each time step an analysis of a small part of the area or space to be covered is carried out and the size of the extension of the buffer zone is based on the average or over all properties of the area to be covered. This requires the models ability to efficiently scan a 2D or 3D polygon efficiently for objects of different resistances.

2.3 2D Model

The basic case for geospatial buffering is well established in two dimensions and hence only requires introduction of our event resistance model. We start by assuming a point source at the origin, having a potential P. This potential can describe the amount of substance available, the pressure, or a number of other parameters depending on the modeled phenomenon. Based on P we assume that a model for how the pressure wave, substance or event propagates. The propagation has two principal features, propagation speed and intensity. The propagation speed v mainly depends on P and the resistance or conductivity of the traversed medium or substance while the intensity I also depends on the distance r from the source. The dependency on the distance from the source will often be proportional to r^{-n}, where n is a positive number. However, this is not always the case, e.g in the case of a fire which may gain energy and speed as larger areas are covered.

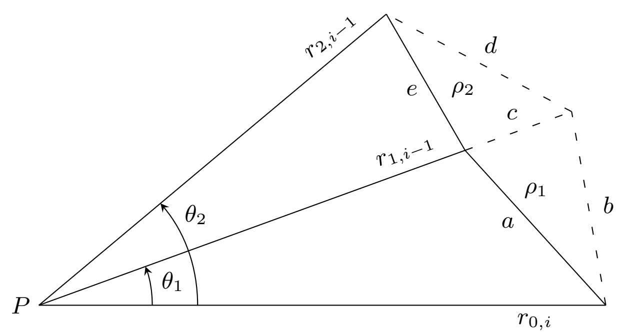

Fig. 1. A section of a 2D buffer

We assume that the buffer surface is continuous but not derivable in all points. As the propagation from the point source goes in straight lines, a polar coordinate system is appropriate, which allows the identification of a specific radian by its angular coordinate and to follow this radian over time. Thus a point in the plane is uniquely determined by (r, θ), where r is the distance from the origin and θ is the angle required to reach the point from the x-axis. Figure 1 shows three radians, the ones with θ equal to 0, $2\pi/N$, and $4\pi/N$, where N is the selected number of partition of the surface. In the sketched scenario the algorithm is about to evaluate $v(P, r_{1,i-1}, \theta_1)$. In order to do this one needs to determine the resistance of the area ahead of the point $(r_{1,i-1}, \theta_1)$, i.e. the polygons abc and cde. We introduce c here, the potential extension of the buffer surface in direction θ_1 given that the resistance would be 0, i.e. $c = v(P, r_{1,i-1}, \theta_1 | \rho = 0)$. This is necessary in order to define the polygons abc and cde. Once the estimate for c is found, ρ_1 and ρ_2, which are the maximum resistances of polygon abc and cde respectively, are determined. Using the maximum metric to determine the resistance of the area is obviously a simplified approach. Another, computationally more expensive, option would be to use a weighted average of resistances based on how much of the polygon area the different objects cover. For now we choose to focus on the creation of the buffer area, contenting ourselves to the maximum metric. Once the resistance of the area is determined, the length of c is adjusted according to equation 1:

$$v(P, r, \rho_1, \rho_2) = \begin{cases} v(P, r) & \text{if } \sum \rho = 0 \\ v(P, r)/2 & \text{if } \sum \rho = 1 \\ 0 & \text{if } \sum \rho = 2. \end{cases} \tag{1}$$

From this we see that if both *abc* and *cde* have high resistance, the propagation in this direction stops abruptly. If only one of these are fire-resistant the propagation continues, but at a lower speed. Obviously the selection of N is an important step; as the length of a circle arc grows as $2\pi r$, the granularity of the partition decays relatively fast, and the accuracy of the result decays at a similar speed. Thus an area of interest must be defined in the scenario description, and over-refinement in the early steps of the computations must be accepted.

2.4 3D Point Buffering

Again we assume a point source, but this time in a three-dimensional space applying the same approach as in the previous section stipulating the maximal extension of one edge of the buffer surface, analyze the resistance of the covered area, and then adjust the extension according to this. Further we want to take advantage of the increased level of detail that a 3D construct can provide, since e.g. gravity is an important factor for many substances and phenomena, which can be included in the expression of v and adjusted according to the angle the velocity has to the xy-plane. Variations in the terrain inclination and air currents can also be captured in this model. Here, spherical coordinates (the 3D analogue to polar coordinates) are chosen for space representation. A location is uniquely determined by the 3-tuple (r, θ, ψ), where r is the distance from the origin to the point, θ is the angle between the positive x-axis and the line from the origin to the point projected onto the xy-plane, and ψ is the angle between the positive z-axis and the line formed between the origin and point. The angular parameters are discretized so that r_{ijk} represent the distance between the source in angular direction (θ_j, ψ_k) in the i-th iteration. As in the two-dimensional case our approach is to analyze the volumes (not the area) in the vicinity of the point of interest on the propagation limit or buffer surface. Figure 2 shows a planar projection of the vicinity point of the surface point $r_{i,0,0}$, and visualizes the discretization of the angles.

We are now to estimate $v(P, r_{i,0,0})$. As in the 2D case we let $c = v(P, r_{i,0,0} | \rho = 0)$. From this we define four volumes in the vicinity of the point of interest, each of form similar to the one sketched in fig. 3, based on the four vicinity grids of fig. 2. Analyzing the resulting volumes we can now determine the resistances $(\rho_1, \rho_2, \rho_3, \rho_4)$ for each volume, and from this adjust the length of c according to equation 2.

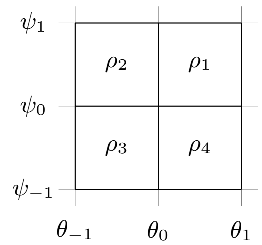

Fig. 2. Planar projection of a 3D buffer surface for point source

$$v(P, r, \theta, \psi, \rho_1, \rho_2, \rho_3, \rho_3) = \begin{cases} v(P, r, \theta, \psi) & \text{if } \sum \rho = 0 \\ \frac{v(P,r,\theta,\psi)}{4} & \text{if } \sum \rho = 1 \\ \frac{v(P,r,\theta,\psi)}{2} & \text{if } \sum \rho = 2 \\ \frac{3v(P,r,\theta,\psi)}{4} & \text{if } \sum \rho = 3 \\ 0 & \text{if } \sum \rho = 4. \end{cases} \tag{2}$$

The references to the angles are kept in order allow the inclusion of features such as gravity and atmospheric features to the model. As in the 2D case we note that again the angular partition has to be considered carefully at the initialization of the model. The area of a spherical surface grows as πr^2 so the granulation becomes a major issue at large distances from the centre. However, amplitudes of event propagation tend to decay at the same or faster speeds.

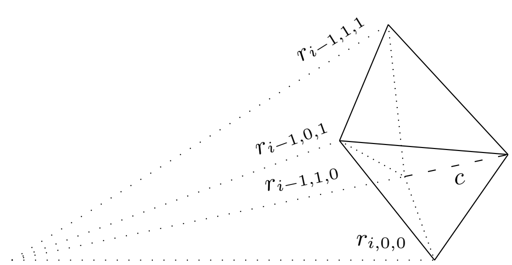

Fig. 3. An extension volume of the 3D buffer for a point source

2.5 3D Line Segment Buffering

A line in three-dimensional space can be defined as two end nodes with zero or more internal nodes. In GIS, line data are used to represent one-dimensional objects such as roads, railroads, canals, rivers and power lines. The straight parts of a line between two successive vertices (internal nodes) or end nodes are called line segments, thus a model for line segment buffering is needed [6]. A line can

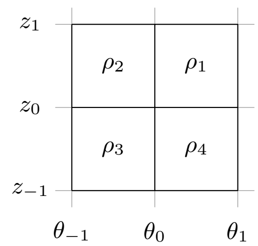

Fig. 4. Planar projection of a 3D buffer surface for segment source

be viewed as a set of points. We assume that the sources are lined up e.g on the z-axis, and choose to focus on spreading in the plane which is normal to the z-axis. This leads to cylindrical coordinates being a well-suited representation for the given scenario. In cylindrical coordinates, a point is defined by the 3-tuple (r, θ, z), where r is the distance of from the point to the z-axis, θ is the angle between the positive x-axis and the line from origin to the point, and z is the z-coordinate of the point. We will use the notation $r_{i,j,k}$ to identify the position of the buffer surface point with z-coordinate x and angular position θ_j in iteration i. The planar projection of the vicinity of a point of interest on the buffer surface is shown in fig. 4. We see that this is much the same as the scheme in fig. 2, only that ψ is replaced by z.

Once the discretization scheme is established, the buffer extension process, visualized in fig. 5, is much the same for line buffering as it was for point buffering, extending $r_{i,j,k}$ as it was in an environment with low resistance, analyzing the extension volumes, and adjusting the extension as a function of these. The adjustment can be done by again using eq. 2, but substituting $v(P, r, \theta, \psi)$ with $v(P, r, \theta, z)$. Again we would like to keep the reference to the position, in order to be able to extend the model with physical features. In this case granularity is less of an issue than in the case of point source. As $z_{i+1} - z_i$ is constant for all iterations, the area of the cylindrical surface grows as $2\pi r$, as in the 2D scenario.

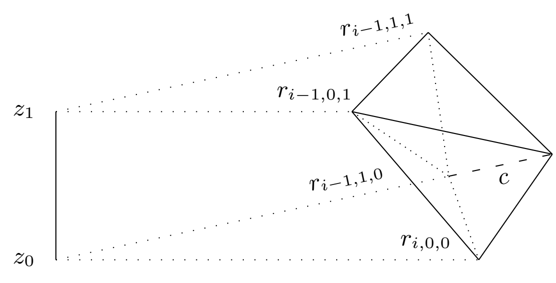

Fig. 5. An extension volume of the 3D buffer for a line segment source

We should also note that we in this approach has omitted the influence that the different sources have on each other, which for small r is not negligible.

2.6 3D Polygon Buffering

Polygons are are the third, and last, class of important objects to be considered. However, here we simply note that this can be achieved with a combination of the techniques previously discussed. The surface can be discretized as a grid while the sides of the surface are extended as line buffers (with propagation as a half-cylinder due to edge effects) and treating the corners as point buffers (with propagation as in a quarter of a sphere if the corner of the surface is a straight angle). Additional side conditions apply, but are omitted here for space reasons.

2.7 Geospatial Data and Physical Features

The different buffering methods has so far been described in very precise locations in the coordinate system. Giving sources, lines and polygons a general location in a coordinate system is merely a question of translations and rotations that can be carried out in a straight forward way, and is not included in our discussions. In order to include geospatial data into the model we propose the use of a local voxel representation of the area of interest. Each voxel is associated with a ρ value. In this way, both geological and infrastructural volume elements can be modeled. A voxel representation in combination with finer granulation of the resistance parameter further allows for finer analysis of the resistance of extension volumes, allowing also for heterogeneous refinement and use of dynamic ρ functions as described above. Physical features such as gravity or air currents can be included as previously mentioned by adding additional conditions on v. The use of spherical and cylindrical coordinates has the advantage of defining the angle of what can be viewed as a velocity vector relative to the perpendicular plane. From this, elementary mechanics can be used to determine the effect of gravity or other external forces on the velocity of the dispersing particles.

3 Example Scenario

As an example of the applicability of the model consider a gas pipeline being located in proximity to a telecommunications exchange. A graph-based model such as the one reported in [1], will not detect direct interdependencies, although it may be possible in some cases to identify indirect, transitive, or even cyclical interdependencies between these heterogeneous infrastructure components. Further infrastructure elements such as a power station may, however, require both of these infrastructure elements to be operational either directly or for risk mitigation (e.g. for signaling imminent failure to a network control station in case of loss of gas pressure). For the threat of a blast emanating from the gas pipeline, it is necessary to perform an analysis that takes the terrain configuration as well as the type of event (a vapor cloud explosion typical of a gas explosion) into account [7, 8]. Such an analysis is only partially achievable using 2D or 2.5D GIS analysis. Assume a scenario as presented in fig. 6 with a point source S of an possible explosion located in the vicinity of two buildings A and B in a city landscape. Building B contains a cellular phone base station T. A 2D simulation of a point source buffer around S, shows that T is protected by the building A.

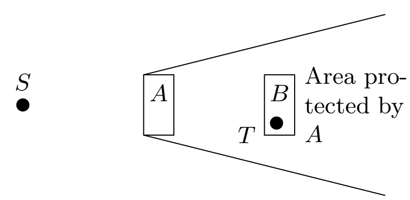

Fig. 6. The result of a 2D or 2.5D simulation

If we now consider a 3D simulation of the same scenario we would have to investigate or collect information regarding the exact location of T also in the vertical direction. Assuming that T is located on the roof of B, and that B is a taller building than A we may very well have a scenario in the xz plane as is sketched in fig. 7. In this case only the lower part of B is protected by A, and we do indeed have a dependency between the infrastructure in S and the infrastructure served by T in this area.

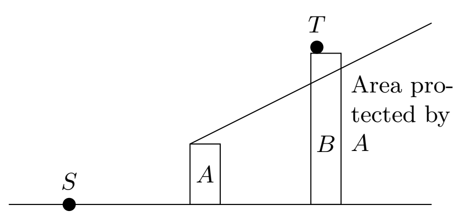

Fig. 7. The result of a 3D simulation seen in a xz section

4 Related Work

Despite the heightened interest in geospatial modeling in general caused largely by the increasing availability of GIS tools to the general public, research on the use of such models and tools has been limited [9, 10]. In part this is also based on both limited availability of three-dimensional geospatial data and also of currently limited support by GIS tools. However, several 3D-capable GIS environments are available, and standardization efforts e.g. on the part of the

OpenGIS consortium are progressing rapidly. GIS approaches using 3D representations have e.g. been proposed for hydrological applications such as flood warning [11] while terrain and topology features have also been used previously in 2D contexts [12]. Patterson and Apostolakis use a Monte Carlo approach based on multi-attribute utility theory to predict locations of interest e.g. to targeted attacks incorporating GIS features and also taking multiple infrastructure types into account [13]. Other proposed application areas for selected critical infrastructures are the integration of geospatial and hydraulic models [14] and the continuity of telecommunications backbone structures [15]. This indicates that critical infrastructure models can benefit greatly from adapting and incorporating selected aspects of geospatial models for specific questions such as blast damage assessments [7, 8] or plume propagation [16, 17].

5 Conclusion

In this paper we have described a localized model for investigating events and configurations of interdependent critical infrastructure elements which takes the geospatial positioning and terrain features into account. Moreover, we have shown that a framework for characterizing properties of geospatial volumes with regard to the permeability to certain events such as fire, flooding, or blasts, can yield approximations useful for risk and threat assessment which may then be refined further in more specialized but also computationally complex models. The model framework described in this paper is intended to supplement and extend the graph-based model reported in [1–4], not to supplant it. A typical application of the model would therefore associate geolocation information with the vertices of the graph-based model and then selectively investigate the geospatial neighborhood of a particular graph vertex or set of vertices of interest to ensure that no hidden dependencies and risks exist that cannot be captured adequately by a purely topological approach. Future work includes more detailed modeling of terrain types as well as of effects of various event types and their interactions with both terrain types and topographical features. This, in conjunction with the integration of 3D polygonal buffering will allow a more detailed investigation of events in complex terrain. However, the availability of sufficiently detailed terrain information in existing GIS databases currently still represents an obstacle to more widespread use, and presently limits our implementation to small models. Moreover, to improve performance it would be highly desirable to for GIS environments to fully support queries such as 3D polygonal buffering, which currently must be performed by the modeling environment.

References

1. Svendsen, N.K., Wolthusen, S.D.: Multigraph Dependency Models for Heterogeneous Infrastructures. In: First Annual IFIP Working Group 11.10 International Conference on Critical Infrastructure Protection, Hanover, NH, USA, IFIP, Springer-Verlag (March 2007) 117–130

2. Svendsen, N.K., Wolthusen, S.D.: Connectivity models of interdependency in mixed-type critical infrastructure networks. Information Security Technical Report **12**(1) (March 2007) 44–55
3. Svendsen, N.K., Wolthusen, S.D.: Analysis and Statistical Properties of Critical Infrastructure Interdependency Multiflow Models. In: Proceedings from the Eighth Annual IEEE SMC Information Assurance Workshop, United States Military Academy, West Point, NY, USA, IEEE Press (June 2007) 247–254
4. Svendsen, N.K., Wolthusen, S.D.: An analysis of cyclical interdependencies in critical infrastructures. Accepted for publication at CRITIS 2007 (October 2007)
5. Worboys, M., Duckham, M.: GIS: A Computing Perspective. Second edn. CRC Press (2004)
6. Khuan, C.T., Rahman, A.A.: Geo-information for disaster management. In van Oosterom, P., Zlatanova, S., Fendel, E.M., eds.: Peter van Oosterom and Siyka Zlatanova and Elfriede M. Fendel, Springer Verlag (2005) 841–865
7. Cleaver, R.P., Humphreys, C.E., Morgan, J.D., Robinson, C.G.: Development of a model to predict the effects of explosions in compact congested regions. Journal of Hazardous Materials **53**(1) (May 1997) 35–55
8. Alonso, F.D., Ferradása, E.G., Sánchez Péreza, J.F., Miñana Aznara, A., Ruiz Gimenoa, J., Martínez Alonso, J.: Characteristic overpressure-impulse-distance curves for vapour cloud explosions using the TNO Multi-Energy model. Journal of Hazardous Materials **137**(2) (September 2006) 734–741
9. Wolthusen, S.D.: Modeling Critical Infrastructure Requirements. In: Proceedings from the Fifth Annual IEEE SMC Information Assurance Workshop, United States Military Academy, West Point, NY, USA, IEEE Press (June 2004) 258–265
10. Wolthusen, S.D.: GIS-based Command and Control Infrastructure for Critical Infrastructure Protection. In: Proceedings of the First IEEE International Workshop on Critical Infrastructure Protection (IWCIP 2005), Darmstadt, Germany, IEEE Press (November 2005) 40–47
11. Stamey, B., Carey, K., Smith, W., Smith, B., Stern, A., Mineart, G., Lynn, S., Wang, H., Forrest, D., Kyoung-Ho, C., Billet, J.: An Integrated Coastal Observation and Flood Warning System: Rapid Prototype Development. In: Proceedings of OCEANS 2006, Boston, MA, USA, IEEE Press (September 2006) 1–6
12. Mladineo, N., Knezic, S.: Optimisation of Forest Fire Sensor Network Using GIS Technology. In: Proceedings of the 22nd International Conference on Information Technology Interfaces (ITI 2000), Pula, Croatia, IEEE Press (June 2000) 391–396
13. Patterson, S.A., Apostolakis, G.E.: Identification of critical locations across multiple infrastructures for terrorist actions. Reliability Engineering & System Safety **92**(9) (September 2006) 1183–1203
14. Pollert, J., Dedus, B., eds.: Real Time Analysis for Early Warning Systems. In: Security of Water Supply Systems: From Source to Tap. Volume 8 of NATO Security through Science Series. Springer-Verlag, Berlin, Germany (2006) 65–84
15. Casey, M.J., ed.: Communications Infrastructure Security: Dynamic Reconfiguration of Network Topologies in Response to Disruption. In: Protection of Civilian Infrastructure from Acts of Terrorism. Volume 11 of NATO Security through Science Series. Springer-Verlag, Berlin, Germany (2006) 231–246
16. Spaulding, M.L., Swanson, J.C., Jayko, K., Whittier, N.: An LNG release, transport, and fate model system for marine spills. Journal of Hazardous Materials **140**(3) (February 2007) 488–503
17. Scollo, S., Carloa, P.D., Coltellia, M.: Tephra fallout of 2001 Etna flank eruption: Analysis of the deposit and plume dispersion. Journal of Vulcanology and Geothermal Research **160**(1–2) (February 2007) 147–164